Contribution from the Department of Chemistry, Emory University, Atlanta, Georgia 30322, and Applied Biosystems, Foster City, California 94404

Multinuclear NMR Investigation of Zn^{2+} Binding to a Dodecamer Oligodeoxyribonucleotide: Insights from ^{13}C NMR Spectroscopy

Xin Jia,[†] Gerald Zon,[‡] and Luigi G. Marzilli*[,†]

Received August 27, 1990

The ^1H and ^{13}C NMR spectra of the self-complementary dodecamer $d(A_1T_2G_3G_4G_5T_6A_7C_8C_9C_{10}A_{11}T_{12})_2$ were assigned. The dodecamer chemical shifts and NOE effects suggest a normal B-form duplex at 12 °C. However, weak NOE cross peaks from the AH2 signal to the H1′ signal of the 3′ nucleotide were observed. These weak cross peaks are consistent with some minor sliding in of the propeller-twisted base pairs, particularly at the center of the duplex. At lower concentrations or at higher temperature, a second form of the oligonucelotide was evident. This concentration dependence, the downfield chemical shifts of some ^1H resonances, and the observation of an imino signal at 11 ppm strongly imply that this minor form is a hairpin. Addition of Zn^{2+} greatly disfavored this hairpin form. At lower oligonucleotide concentration, Zn^{2+} was twice as effective as Mg^{2+} in favoring the duplex form. The imino ^1H spectra established that GC base pairing is not disrupted in the duplex form, even at high levels of added Zn^{2+}. At higher oligonucleotide concentration, when the duplex was converted to the random coil form by temperature elevation, no hairpin form was detected in the presence of Zn^{2+}, whereas such a form was clearly present, particularly at 42 °C, in the absence of Zn^{2+}. At low temperature, when Zn^{2+} was added, the H8 signals at G_4 and, to a lesser extent, G_3 shifted downfield with little effect on the G_5H8 or any AH8 signals. This result suggests a preferential binding to N7 of G4. This conclusion was strongly supported by downfield shifts of the G_4 and G_3 C8 signals and the absence of appreciable changes in the C8 signals of other purines. In addition, the C5 signals of G_4 and G_3 shifted upfield and the C4 signals broadened. These characteristic changes strongly support coordination to N7 for these two G residues. However, no significant changes in NOE cross-peak intensities, the C3′ ^{13}C signals, or the ^{31}P NMR signals were observed. Therefore, it is clear that GN7-M-GN7 cross-linked or GMG sandwich species are not formed, since the strain in the sugar-phosphate backbone that would be produced by such species would have led to appreciable changes in chemical shift and NOE cross-peak intensity. The selectivity pattern ($G_4 > G_3 > G_5$, A) is consistent with the expected molecular electrostatic potential on the basis of literature calculations. Thus, although the study of spectroscopically silent labile metal ions such as Zn^{2+} is difficult, a multinuclear NMR investigation of the target biomolecule can be quite revealing.

Introduction

The importance of metal ion interactions with nucleic acids has been recognized for some time.[1,2] Metal ions influence DNA structure and stability.[1,2] Metal atoms are found in antitumor drugs that act at the DNA level,[3] in DNA binding proteins,[4] in RNA and DNA processing enzymes,[5] and in conformational and structural probes of DNA and RNA.[6] Synthetic oligonucleotides have become extremely useful models for studying interactions of small molecules with DNA by NMR spectroscopy.[7-10] Most of the NMR spectroscopic studies of binding of metal species to oligonucleotides have involved Pt(II) compounds.[8] Other metal complexes, such as metalloporphyrins[9] and inert octahedral complexes used as DNA conformational probes[10] have been studied by NMR spectroscopy to a lesser extent. A useful backdrop for a complete understanding of the binding of these types of species to DNA would be a better understanding of how simple metal ions bind to DNA and influence DNA structure and stability. Most of the NMR studies of oligonucleotides reported to date have involved 1D and 2D ^1H NMR and some 1D ^{31}P and 2D ^1H-^{31}P NMR studies.[7-10] Although ^1H NMR spectroscopy has played an important role in identifying metal binding sites to nucleosides and nucleotides, ^{13}C NMR spectroscopy can be very informative, since distinct patterns of upfield and downfield shifts for heterocyclic base ^{13}C signals are one of the most unambiguous methods of defining metal binding sites in solution.[11]

Recent studies have shown that ^{13}C NMR spectroscopy of oligonucleotides is quite feasible,[12] and other studies have suggested that sugar pucker (S vs N) can be readily determined on the basis of ^{13}C shifts—particularly of the C3′ signal.[13] We report here one of the first attempts to utilize ^{13}C NMR spectroscopy of oligonucleotides to understand metal ion binding. We have also used 1D and 2D ^1H NMR and 1D ^{31}P spectroscopy to probe the binding of Zn^{2+} to an oligonucleotide.

We selected Zn^{2+} for study for several reasons. It is the metal found most often in DNA binding proteins[4] and in enzymes involved in DNA and RNA biochemistry.[5] Also, Zn^{2+} has one of the most interesting groups of effects on DNA unwinding and rewinding of all of the simple divalent metal ions.[1,14-16] Of additional interest, Zn^{2+}-DNA interactions are characteristic of

† Emory University.
‡ Applied Biosystems.

(1) Eichhorn, G. L. In *Inorganic Biochemistry*; Eichhorn, G. L., Ed.; Elsevier Scientific Publishing Co.: Amsterdam, 1973; Vol. 2, p 1210.
(2) Eichhorn, G. L. In *Advances in Inorganic Biochemistry*; Eichhorn, G. L.; Marzilli, L. G., Eds.; Elsevier North-Holland, Inc.: New York, 1981; Vol. 3, p 1.
(3) Leh, F. K. V.; Wolf, W. *J. Pharm. Sci.* **1976**, *65*, 315. Reedijk, J.; Fichtinger-Schepman, A. M. J.; van Oosterom, A. T.; van de Putte, P. *Struct. Bonding* **1987**, *67*, 53. Johnson, N. P.; Butour, J.-L.; Villani, G.; Wimmer, F.; Defais, M.; Pierson, V.; Brabec, V. *Progress in Clinical Biochemistry and Medicine*; Springer-Verlag: Berlin, 1989; Vol. 10, p 1. Griffin, J. H.; Dervan, P. B. *J. Am. Chem. Soc.* **1987**, *109*, 6840 and references cited therein. Gao, X.; Patel, D. *Q. Rev. Biophys.* **1989**, *22*, 93. Stubbe, J.; Kozarich, J. W. *Chem. Rev.* **1987**, *87*, 1107.
(4) O'Halloran, T. V. In *Advances in Inorganic Biochemistry*; Eichhorn, G. L.; Marzilli, L. G., Eds.; Elsevier: New York, 1990; Vol. 8, p 1. Summers, M. F. In *Advances in Inorganic Biochemistry*; Eichhorn, G. L., Marzilli, L. G., Eds.; Elsevier: New York, 1990; Vol. 8, p 199. Summers, M. F.; South, T. L.; Kim, B.; Hare, D. R. *Biochemistry* **1990**, *29*, 329. Lee, M. S.; Gippert, G. P.; Soman, K. V.; Case, D. A.; Wright, P. E. *Science* **1989**, *245*, 635. Pan, T.; Coleman, J. E. *Biochemistry* **1990**, *29*, 3023.
(5) Shishido, K.; Ando, T. In *Nucleases*; Linn, S. M., Roberts, R. J., Eds.; Cold Spring Harbor Laboratory: Cold Spring Harbor, NY 1982; p 23. Vogt, V. M. *Eur. J. Biochem.* **1973**, *33*, 192. Mayaux, J. F.; Blanquet, S. *Biochemistry* **1981**, *20*, 4647.
(6) Chow, C. S.; Barton, J. K. *J. Am. Chem. Soc.* **1990**, *112*, 2839. Mei, H.-Y.; Barton, J. K. *Proc. Natl. Acad. Sci. U.S.A.* **1988**, *85*, 1339. Hiort, C.; Norden, B.; Rodger, A. *J. Am. Chem. Soc.* **1990**, *112*, 1971. Ryle, A. M.; Long, E. C.; Barton, J. K. *J. Am. Chem. Soc.* **1989**, *111*, 4520. Chen, C.-h. B.; Sigman, D. S. *J. Am. Chem. Soc.* **1988**, *110*, 6570. Yoon, C.; Kuwabara, M. D.; Spassky, K. A.; Sigman, D. S. *Biochemistry* **1990**, *29*, 2116. Youngquist, R. S.; Dervan, P. B. *J. Am. Chem. Soc.* **1987**, *109*, 7564.
(7) Scott, E. V.; Zon, G.; Marzilli, L. G.; Wilson, W. D. *Biochemistry* **1988**, *27*, 7940. Gao, X.; Patel, D. J. *Biochemistry* **1988**, *27*, 1744. Marzilli, L. G.; Banville, D. L.; Zon, G.; Wilson, W. D. *J. Am. Chem. Soc.* **1986**, *108*, 4188. Wilson, W. D.; Jones, R. L.; Zon, G.; Banville, D. L.; Marzilli, L. G. *Biopolymers* **1986**, *25*, 1997.
(8) Caradonna, J. P. Lippard, S. J. *Inorg. Chem.* **1988**, *27*, 1454 and references cited therein. Neumann, J.-M.; Tran-Dinh, S.; Girault, J.-P.; Chottard, J.-C.; Huynh-Dinh, T.; Igolen, J. *Eur. J. Biochem.* **1984**, *141*, 465. Kline, T. P.; Marzilli, L. G.; Live, D.; Zon, G. *J. Am. Chem. Soc.* **1989**, *111*, 7057 and references cited therein. Fouts, C. S.; Marzilli, L. G.; Byrd, R. A.; Summers, M. F.; Zon, G.; Shinozuka, K. *Inorg. Chem.* **1988**, *27*, 366. den Hartog, J. H. J.; Altona, C.; van Boom, J. H.; van der Marel, G. A.; Haasnoot, C. A. G.; Reedijk, J. *J. Biomol. Struct. Dyn.* **1985**, *2*, 1137.

0020-1669/91/1330-0228$02.50/0 © 1991 American Chemical Society

those of other simple ions in many ways,[16] and if we can understand its binding, we will thereby gain considerable insight into the binding of other labile metal ions such as Cu^{2+}. In contrast to Cu^{2+} and other 3d divalent transition-metal ions, Zn^{2+} is diamagnetic; the diamagnetism simplifies the interpretion of the NMR studies. Finally, the labile, diamagnetic Zn^{2+} will bind at the thermodynamically favorable site. Excluding steric effects, this site should be the position of most favorable electrostatic potential in the DNA major groove. Considerable effort has been expended on theoretical calculations that will give insight into these potentials.[17] Such calculations provide estimates of GN7 nucleophilicity, which can also probed experimentally with alkylating agents.[18] The binding of alkylating agents is thermodynamically irreversible. Alkylation site preference is kinetically controlled, and therefore additional methods for assessing DNA surface charge would be useful. Nevertheless, such alkylation studies have additional importance, e.g. alkylation has transformation-inducing properties by means of a mutation that affords an activated oncogene.[18]

Our findings are best discussed in terms of previous suggestions about metal binding modes to DNA polymers. Considerable indirect evidence exists that Zn^{2+} and other metal ions such as Cu^{2+}, Mn^{2+}, Cd^{2+}, Co^{2+}, etc. bind to the GC base pairs, since the effects of these metals increase with DNA GC content.[14,15,19] It is widely believed that the preferred binding site is N7 of G.[15] However, there are many suggestions that the metal ion may cross-link adjacent bases, such as two guanines, or that chelate complexes are formed involving N7 and a phosphate group.[15,19] The UV spectral changes that have been observed have been attributed to the partial transfer of the imino proton on N1 of G to N3 of C (namely, an alteration in the Watson–Crick base pairing scheme resulting from the binding of an electrophilic metal ion to N7). CD spectral changes have been attributed to global conformational changes brought about by metal ion binding.[15]

Metal ions also influence the thermal denaturation of DNA and can either increase or decrease the midpoint temperature (T_m) of the duplex-to-coil transition.[1,2,14,19] It has been suggested that only AT base pairs are involved in the denaturation process.[19] Also, metal ions may possibly prevent the formation of structures such as hairpins, which normally impede renaturation of DNA.[20] We have suggested that the prevention of hairpin formation by Zn^{2+} could explain at least partly the ability of this ion to facilitate renaturation of DNA.[16] At low concentrations, most metal ions increase T_m, but at higher concentrations some metal ions, such as Zn^{2+}, Cu^{2+}, and Cd^{2+}, decrease T_m.[12,14] Such a decrease could result from stabilization of the random coil form.

We have found that NMR studies of oligonucleotides, particularly using ^{13}C NMR, can be very informative in improving our understanding of metal ion binding to DNA. Unambiguous support or clear refutation of some of these suggested interactions has resulted from our studies.

Experimental Section

Sample Preparations. The oligodeoxyribonucleotide (oligomer) (5′ → 3′)d(ATGGGTACCCAT)$_2$ was synthesized and purified as previously described.[21] Zn^{2+}–oligomer samples were prepared by adding the correct amount of $ZnCl_2$ stock solution to the solution of the oligomer and adjusting the pH to 6.00. The Zn^{2+} stock solution was prepared by weighing an appropriate amount of $ZnCl_2$ into a 50-mL volumetric flask and adding 2 small drops of 5.5 M HCl and then deionized water. The solution concentration, 0.1 M, was determined by atomic absorption spectroscopy. Samples were lyophilized and then dissolved in 0.5 mL of 99.96% D_2O, and the solutions were transferred (under nitrogen) to 5-mm NMR tubes.

Extinction Coefficient Determination. The "near-neighbor" method[22] was employed to calculate ϵ_{260av}, the average value per base in the absence of base stacking. Then the absorbance at 260 nm of the oligomer solution was recorded at 92 and 25 °C. From the equation $\epsilon_{260(25^\circ C)} = (A_{25^\circ C}/A_{92^\circ C})\epsilon_{260av}$, the value of ϵ_{260} at 25 °C was calculated to be 7490 M^{-1} cm^{-1} per base.

^1H and ^{13}C NMR Spectroscopy. ^1H NMR experiments were performed at 500.10 MHz except as noted on a GE GN-500 spectrometer with a variable-temperature controller. The following experiments were performed at 12 °C except where noted.

One-dimensional proton spectra were recorded typically with 5000-Hz sweep width, 30° pulse width, and 16K data points for D_2O samples and 8000-Hz sweep width, 80° pulse width, 16K data points, and 1331 solvent suppression sequence with a presaturation pulse for 90% H_2O/10% D_2O samples. For NOE difference spectra, 128 scans collected with the saturating field directed off-resonance were subtracted from an equal number of scans with the saturating field on-resonance. No internal standard was added. The chemical shift calibration was based on the signal of residual HOD.

2D homonuclear *J*-correlation spectroscopy (COSY)[23] with presaturation and ^{31}P decoupling (1-W power) at 202.443 MHz resulted from a 512 × 2048 data matrix size with 16 scans per t_1. A sweep width of 5000 Hz and a 1.3-s delay time between scans were used.

Phase-sensitive 2D cross-relaxation correlation (NOESY) and chemical exchange correlation spectroscopy (EXSY) experiments both used the same pulse sequence[24,25] with presaturation and ^{31}P decoupling. For these experiments a 512 × 2048 data matrix size was used with 16 scans per t_1. A 3-s delay between scans and a 5000-Hz sweep width were used. Mixing times used in two NOESY experiments were 100 and 300 ms. A 300-ms mixing time was used in the EXSY experiment at 42.5 °C.

The COSY and NOESY spectra as well as other 2D spectra were processed with the FTNMR program (Hare Research, Inc., Woodinville, WA). The data were apodized with a Gaussian sine function in both dimensions. In the t_1 dimension the data were zero-filled once before Fourier transformation.

Heteronuclear multiple quantum correlation (HMQC) and phase-sensitive HMQC (PHMQC)[26] spectra resulted from a 128 × 1024 data

(9) Strickland, J. A.; Marzilli, L. G.; Wilson, W. D.; Zon, G. *Inorg. Chem.* **1989**, *28*, 4191.
(10) Rehmann, J. P.; Barton, J. K. *Biochemistry* **1990**, *29*, 1701, 1710.
(11) Marzilli, L. G.; Stewart, R. C.; Van Vuuren, C. P.; de Castro, B.; Caradonna, J. P. *J. Am. Chem. Soc.* **1978**, *100*, 3967. Marzilli, L. G.; de Castro, B.; Caradonna, J. P.; Stewart, R. C.; van Vuuren, C. P. *J. Am. Chem. Soc.* **1980**, *102*, 916. Marzilli, L. G.; de Castro, B.; Solorzano, C. *J. Am. Chem. Soc.* **1982**, *104*, 461. Marzilli, L. G. *Progress in Inorganic Chemistry*; Lippard, S. J., Ed.; Wiley-Interscience: New York, 1977; Vol. 23, p 255.
(12) LaPlante, S. R.; Boudreau, E. A.; Zanatta, N.; Levy, G. C.; Borer, P. N.; Ashcroft, J.; Cowburn, D. *Biochemistry* **1988**, *27*, 7902. Ashcroft, J.; LaPlante, S. R.; Borer, P. N.; Cowburn, D. *J. Am. Chem. Soc.* **1989**, *111*, 363. Borer, P. N.; LaPlante, S. R.; Zanatta, N.; Levy, G. C. *Nucleic Acids Res.* **1988**, *16*, 2323. Borer, P. N.; Ashcroft, J.; Cowburn, D.; Levy, G. C.; Borer, P. N. *J. Biomol. Struct. Dyn.* **1988**, *5*, 1089. Zanatta, N.; Borer, P. N.; Levy, G. C. *Recent Advances in Organic NMR Spectroscopy*; Lambert, J. B.; Rittner, R., Eds.; Norell: Landisville, NJ, 1987; p 89. Live, D. In *Frontiers of NMR in Molecular Biology*; Live, D.; Armitage, I. M.; Patel, D., Eds.; Wiley-Liss: New York, 1990; p 259.
(13) Santos, R. A.; Tang, P.; Harbison, G. S. *Biochemistry* **1989**, *28*, 9372. Borer, P. N.; Zanatta, N.; Holak, T. A.; Levy, G. C.; van Boom, J.; Wang, A. H.-J. *J. Biomol. Struct. Dyn.* **1984**, *1*, 1373. Lankhorst, P. P.; Erkelens, C.; Haasnoot, C. A. G.; Altona, C. *Nucleic Acids Res.* **1983**, *11*, 7215.
(14) Shin, Y. A.; Eichhorn, G. L. *Biochemistry* **1968**, *7*, 1026. Eichhorn, G. L. Shin, Y. A. *J. Am. Chem. Soc.* **1968**, *90*, 7323. Eichhorn, G. L.; Berger, N. A.; Butzow, J. J.; Clark, P.; Rifkind, J. M.; Shin, Y. A.; Tarien, E. *Adv. Chem. Ser.* **1971**, *No. 100*, 135. Shin, Y. A.; Heim, J. M.; Eichhorn, G. L. *Bioinorg. Chem.* **1972**, *1*, 149.
(15) Zimmer, Ch.; Luck, G.; Triebel, H. *Biopolymers* **1974**, *13*, 425.
(16) Jia, X.; Marzilli, L. G. *Biopolymers*, in press.
(17) Aida, M.; Nagata, C. *Int. J. Quantum Chem.* **1986**, *29*, 1253. Sarai, A.; Mazur, J.; Nussinov, R.; Jernigan, R. L. *Biochemistry* **1988**, *27*, 8498. Lavery, R.; Pullman, A.; Pullman, B. *Theor. Chim. Acta* **1982**, *62*, 93. Pullman, A.; Pullman, B. *Q. Rev. Biophys.* **1981**, *14*, 289.
(18) Kohn, K. W.; Hartly, J. A.; Mattes, W. B. *Nucleic Acids Res.* **1987**, *15*, 10531. Wurdeman, R. L.; Church, K. M.; Gold, B. *J. Am. Chem. Soc.* **1989**, *111*, 6408 and references cited therein.
(19) Richard, H.; Schreiber, J. P.; Daune, M. *Biopolymers* **1973**, *12*, 1.
(20) Cantor, R. C.; Schimmel, P. R. In *Biophysical Chemistry, Part III*; W. H. Freeman: New York, 1980; p 1220.
(21) Stec, W. J.; Zon, G.; Egan, W.; Byrd, R. A.; Phillips, L. R.; Gallo, K. A. *J. Org. Chem.* **1985**, *50*, 3908.
(22) Harte, R. A. In *Handbook of Biochemistry*; Harte, R. A., Ed.; The Chemical Rubber Co.: Cleveland, OH, 1968; p 589.
(23) Aue, W. P.; Bartholdi, E.; Ernst, R. R. *J. Chem. Phys.* **1976**, *64*, 2229. Bax, A.; Freeman, R. *J. Magn. Reson.* **1981**, *4*, 542.
(24) Jeener, J.; Meier, B. H.; Bachmann, P.; Ernst, R. R. *J. Chem. Phys.* **1979**, *71*, 4546. Kumar, A.; Ernst, R. R.; Wüthrich, K. *Biochem. Biophys. Res. Commun.* **1980**, *95*, 1.
(25) States, D. J.; Haberkorn, R. A.; Ruben, D. J. *J. Magn. Reson.* **1982**, *48*, 286.
(26) Müller, L. *J. Am. Chem. Soc.* **1979**, *101*, 4481. Bax, A.; Subramanian, S. *J. Magn. Reson.* **1986**, *67*, 565.

matrix size with 512 scans and a 1.1-s delay between scans. A 5000-Hz sweep width was used for the ^1H dimension, and a 8065-Hz sweep width was used for the ^{13}C dimension (frequency = 125.76 MHz). Forty-one watts of ^{13}C rf power and a 38-μs 90° pulse width were used. Since the sweep width used in the carbon dimension was much narrower than the entire carbon chemical shift range, and the pulse was centered in the spectral window, allowance was made for foldover for the AC2, AC8, GC8, TC6, CC6, and T methyl signals. The FID's were apodized with double-exponential multiplication, right-shifted one point and zero-filled prior to the last Fourier transformation. The offset in the carbon dimension was calculated from the absolute frequency of residual HOD ($f^{abs}{}_{^1H}$) taken to be 4.90 ppm relative to TSP ($(CH_3)_3SiCD_2CD_2COONa$) at 12 °C. The frequency (Hz) of HOD relative to TSP ($f^{TSP}{}_{^1H}$) should be

$$f^{TSP}{}_{^1H} = (F1SF + f^{abs}{}_{^1H}) - (4.90 \times 10^{-6})F1SF$$

where F1SF is the ^1H pulse frequency (500.1 MHz). The frequency of ^{13}C relative to TSP can be calculated in a way similar to the method previously used[27] for ^{15}N:

$$f^{TSP}{}_{^{13}C} = f^{atn}{}_{^{13}C} + f^{atn}{}_{^{13}C}/f^{atn}{}_{^1H}(f^{TSP}{}_{^1H} - f^{atn}{}_{^1H})$$

where $f^{atn}{}_{^1H}$ = 500.097 478 MHz and $f^{atn}{}_{^{13}C}$ = 125.749 263 MHz were measured by Prof. David Live. The ^{13}C offset can therefore be obtained by subtracting $f^{TSP}{}_{^{13}C}$ from the ^{13}C frequency used in the experiment.

Selective heteronuclear multiple bond correlation (SHMBC) spectra[28] were obtained by selectively irradiating only the base protons by using the decoupling coil instead of the transmitter coil. Data were collected at 500.1013 MHz for ^1H by using a 128 × 512 data matrix size with 1024 scans per t_1. An 800-Hz sweep width was used for the ^1H dimension, and an 8000-Hz sweep width was used for the ^{13}C dimension (125.77 MHz). Forty-one watts of ^{13}C rf power and a 38-μs 90° pulse width were used. Foldover, not present in the ^1H dimension, was a concern in the ^{13}C dimension for the signals of CC4 and TC4 for the same reason as in HMQC experiment. Double-exponential apodization was used in both dimensions. The data were zero-filled once before Fourier transformation in the t_1 dimension. The offset calculation was the same as that used for the HMQC spectra.

^{31}P NMR Spectroscopy. One-dimensional ^{31}P NMR spectra were recorded at 146.134 MHz with a Nicolet 360-NB spectrometer equipped with a variable-temperature unit. Parameters used include the following: 1400 Hz sweep width, 60° pulse width, broad-band ^1H decoupling, 16K data points, 500-ms delay between scans, and from 1000 to 10 000 scans. The samples, contained in 5-mm NMR tubes, were placed in a 10-mm NMR tube containing D_2O with TMP ($(CH_3O)_3PO$ from Aldrich) as reference.

Results

Assignments by means of 2D NMR methods of d-$(ATGGGTACCCAT)_2$ NMR signals as well as the corresponding signals of the Zn^{2+} complex were made for imino and most nonexchangeable protons and most of the carbons. Since the oligomer duplex is self-complementary, only one strand is of concern. Each nucleoside is referred to according to the following numbering scheme:

$$5'\text{-}dA_1T_2G_3G_4G_5T_6A_7C_8C_9C_{10}A_{11}T_{12}\text{-}3'$$

Concentrations are given in total oligonucleotide bases. Thus, a solution 40 mM in bases corresponds to 3.33 mM in strands or 1.67 mM in duplex. Since under some conditions hairpins or hairpin/duplex mixtures are formed, we have given the concentration throughout in total bases.

Nonexchangeable Proton Assignments. A contour plot of the NOESY spectrum at 300-ms mixing time of free d-$(ATGGGTACCCAT)_2$ is presented in Figure 1. The boxes labeled a–g correspond to the following correlations respectively: (a) aromatic protons to H1′ and CH6 to CH5; (b) aromatic protons to H3′, H4′, H5′, and H5″; (c) aromatic protons to H2′, H2″, and TCH_3; (d) H1′ to H2′, H2″, and TCH_3; (e) H1′ to H3′, H4′, H5′, and H5″; (f) TCH_3 protons to H2′ and H2″; (g) H2′ to H2″ in the same sugar. The correlations of H2′ and H2″ to H3′, H4′, H5′, and H5″ between 1–3 ppm in one dimension and 4–5 ppm in the other dimension overlap severely and were not

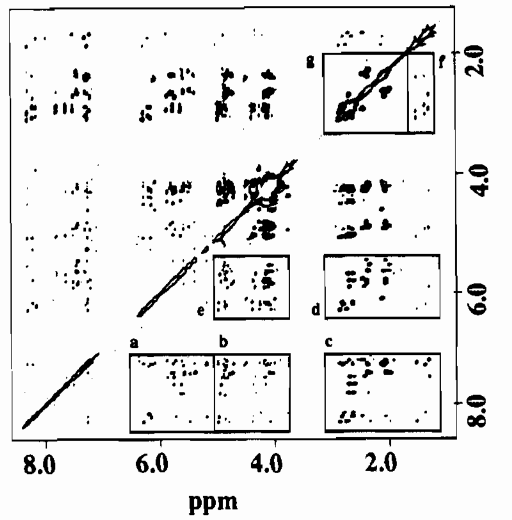

Figure 1. 500.10-MHz ^1H 2D phase-sensitive NOESY (300-ms mixing time) contour plot of $d(ATGGGTACCCAT)_2$ duplex (40 mM in bases) in D_2O, pH 6.0 (uncorrected) at 12 °C.

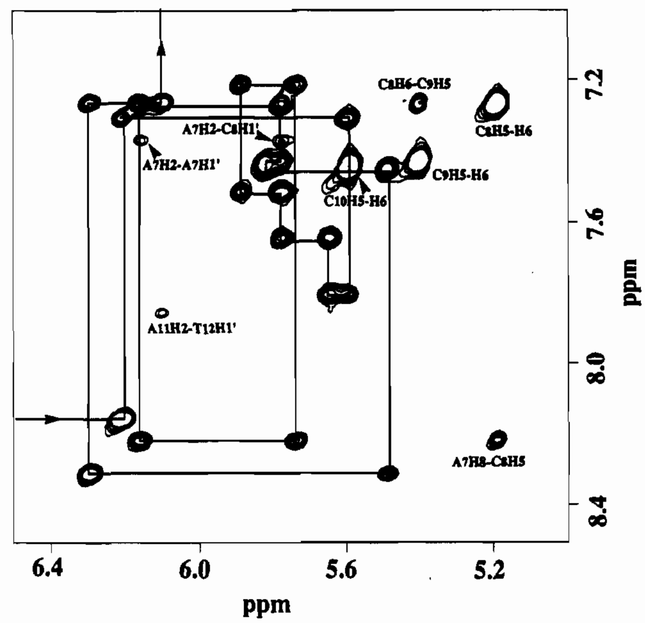

Figure 2. Expanded NOESY spectrum of the H8/H6/H2 to H1′/H5 region of $d(ATGGGTACCCAT)_2$. The sequential H8/H6 to H1′ connectivities from the 5′-end (A_1) to the 3′-end (T_{12}) are connected by solid lines. Internucleotide cross peaks are labeled, as are the CH6 to CH5 intranucleotide NOE cross peaks.

very useful for assignment purposes.

For a B-form duplex, sequential assignments are possible because of the short distances between H1′ and the base proton in its own nucleotide or in the nucleotide in the 3′-direction. Except at the ends, two NOE cross peaks should be seen from every H1′ to two aromatic protons and, from every aromatic proton, two NOE's should be seen to two H1′ signals. The 5′-end aromatic proton signal should have a connectivity to one H1′ and the 3′-end H1′ should have a connectivity to one aromatic proton signal. Figure 2 contains the expanded spectrum of the aromatic proton to H1′ region (a). The sequential connectivity from the 5′-end (A_1) to the 3′-end (T_{12}) or vice versa is indicated by lines. By this procedure aromatic H8, H6, and sugar H1′ signals can be assigned. NOE correlations between H8/H6 and H5 can also be seen, assigning the H5 signals. The three strongest cross peaks in this region are between H5 and H6 of the three cytosine residues. These latter connectivities are also present in the COSY spectrum. Of some interest, some unusual NOE connectivities between AH2 and H1′ of the next residue in the 3′-direction are found, such as $A_7H2\text{-}C_8H1'$ and $A_{11}H2\text{-}T_{12}H1'$. Furthermore,

(27) Live, D. H.; Davis, D. G.; Agosta, W. C.; Cowburn, D. *J. Am. Chem. Soc.* **1984**, *106*, 1939.
(28) Bax, A.; Summers, M. F. *J. Am. Chem. Soc.* **1986**, *108*, 2093.

Table I. ^{1}H Chemical Shifts (ppm) of Signals of d(ATGGGTACCCAT)$_2$ That Change Significantly on Addition of Zn^{2+}

protons	Zn^{2+}/duplex		
	0	3	8
T_2H6	7.33	7.35	7.39
G_3H8	7.83	7.85	7.88
G_4H8	7.67	7.83	7.87
T_6H6	7.24	7.31	7.32
$A_{11}H2$	7.88	7.84	7.83
G_3H1'	5.67	5.90	5.91
$C_{10}H1'$	5.51	5.59	5.58
G_3H2'	2.64	2.60	2.63
G_3H2''	2.72	2.79	2.81
G_4H2'	2.62	2.65	2.68
G_4H2''	2.70	2.65	2.68
$C_{10}H2'$	2.02	2.14	2.17
$C_{10}H2''$	2.45	2.37	2.39
G_4H3'	4.96	4.92	4.97
G_5H3'	4.85	4.80	4.81
$C_{10}H4'$	4.08	4.13	4.15
T_2CH_3	1.40	1.38	1.33
T_6CH_3	1.33	1.34	1.37

one sees an unusual connectivity between A_7H2 and A_7H1' (Figure 2). Assignments are summarized in Table SI (supplementary material).

On the basis of the H1′ assignments, the adjacent H2′ and H2″ can be identified (region d in Figure 1). To further confirm the identification of H2′ and H2″ signals as belonging to a specific sugar, region c in Figure 1 can be used. Aromatic signals not only exhibit cross peaks to the H2′ and H2″ signals of the same nucleotide, but also to H2′/H2″ signals of the next sugar in the 5′-direction. The latter have lower intensity for a B-form duplex. In region g in Figure 1, cross peaks directly indicate which two signals (H2′ and H2″) are for the same ribose. COSY spectra also help with this identification. In the specific assignment of H2′ and H2″ signals, the short mixing time (100 ms) NOESY experiment, where spin diffusion is not as important, is necessary. Since H2″ is always closer to H1′ than H2′, the H2″–H1′ NOE cross peak is stronger than that for H2′–H1′. We found that all the clearly resolved H2″ signals are downfield to the corresponding H2′ signal (Table SI (supplementary material)).

Assignment of the H3′ signals from the NOE cross peaks to either aromatic or H1′ signals is quite straightforward (regions b or e in Figure 1). While, in principle, H4′, H5′, and H5″ assignments can be made through H1′ connectivities, region e is too crowded and the assignments are difficult. The H4′ assignments in Table SI were confirmed by HMQC C4′ assignments discussed below.

From regions c and f in Figure 1, the TCH_3 signals were assigned. These assignments were confirmed with the COSY spectrum.

The A_7H2 and $A_{11}H2$ signals were assigned by the NOESY (300 ms) connectivities of $A_7H2–C_8H_1'$ and $A_{11}H2–T_{12}H1'$. The AH2 assignments were confirmed by 1D NOE experiments discussed below. By difference, A_1H2 was assigned.

The proton signal assignments of the Zn^{2+}–oligomer complexes were made by the same methods (see Tables SII and SIII of the supplementary material). The significant chemical shift changes induced by Zn^{2+} are listed in Table I. It is noteworthy that in the presence of 3 Zn^{2+}/duplex, most of the shift changes have occurred; only small additional changes accompany the addition of more Zn^{2+}. The most significant changes of the aromatic signals involve G_4, where G_4H8 shifted downfield by 0.16 ppm. The G_4 H2′–H2″ signals are no longer resolved. G_3H1' shifted downfield by 0.23 ppm and the G_3 H2′–H2″ resolution increased from 0.08 to 0.19 ppm.

Compared to the significant effect of Zn^{2+} on the chemical shifts, the relative intensities of NOE cross peaks do not change significantly in the 3 Zn^{2+}/duplex spectrum. However, since the

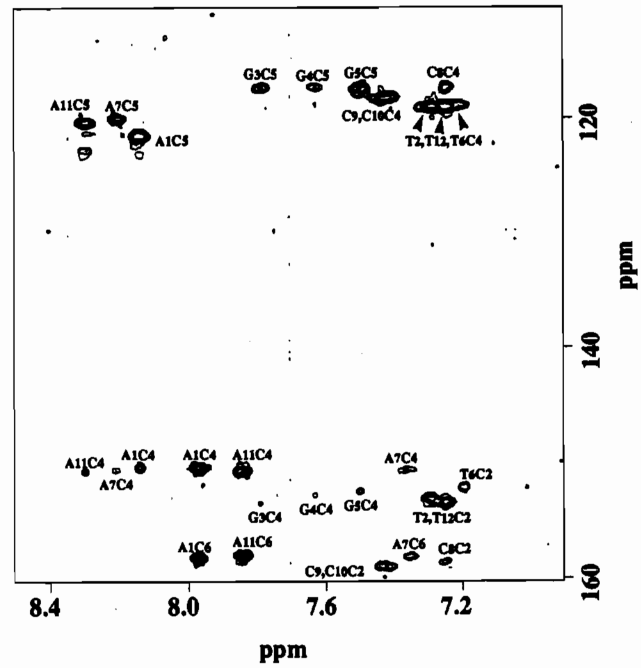

Figure 3. Selective 2D HMBC contour plot of d(ATGGGTACCCAT)$_2$ (40 mM in bases) in D_2O, pH 6.0 (uncorrected) at 12 °C.

data collection and processing were exactly the same for all spectra, some small intensity changes can be detected by a careful examination. For example, the $A_7H2–C_8H1'$ and $G_3H8–T_2H_2'$ cross peaks are stronger than in the spectrum recorded with no Zn^{2+} added, while the $A_{11}H2–T_{12}H1'$ cross peak is weaker. New very weak cross peaks, $A_1H2–T_2H1'$ and $C_8H5–C_9H6$, appear in the presence of Zn^{2+}.

The Zn^{2+} was added to 8 Zn^{2+}/duplex, the limit of solubility at this concentration. The 2D ^{1}H NMR spectra obtained were quite similar to those of the 3 Zn^{2+}/duplex solution except the chemical shifts continued to change, although not by very much (Table SIII (supplementary material)). No further significant NOE intensity changes were found.

^{13}C Assignments. The ^{13}C assignments were made through the use of signals of protons that are connected directly by one bond (HMQC method) or indirectly by two or three bonds but still coupled (HMBC method). Tables II and III give the ^{13}C assignments without and with Zn^{2+}. The assignment is based on the proton assignments. In the HMQC experiment, each ^{1}H signal is split into a doublet (by ~150 Hz) by ^{13}C coupling. By this method, most of the protonated ^{13}C signals, both for the bases (AC2, AC8, GC8, TC6, TCH_3, CC5, and CC6) and sugars (C1′, C3′, and C4′), can be assigned (Table II). Since most of the assignments of H5′ and H5″ were not made, the C5′ assignments were not possible, except for A_1. The C2′ region is too crowded (each H2′ and H2″ signal is split, thus each C2′ has four cross peaks) to be assigned.

In the study of the Zn^{2+} adducts, 1 and 8 Zn^{2+}/duplex were added in separate HMQC experiments (Figure S1 (supplementary material)). Most of the ^{13}C signals of the protonated carbons of the 1 Zn^{2+}/duplex sample were assigned (Table II). Since Zn^{2+} severely broadens some of the ^{13}C signals, the sugar carbon signals in the 8 Zn^{2+}/duplex sample are so broad and overlapped that many assignments were not possible.

From the selective HMBC experiment of the free oligomer (Figure 3), the assignments of most nonprotonated carbons, such as CC2, CC4, TC2, TC4, GC4, GC5, AC4, AC5, and AC6 can be obtained (Table III). However, since no nonexchangeable proton is within three bonds, the assignments of GC2 and GC6 cannot be made. In the presence of 4.5 Zn^{2+}/duplex, most of the nonprotonated carbons were assigned except that some GC4 and GC5 signals were too broad to observe.

The data in the absence of Zn^{2+} in Tables II and III can be used to contrast the assignments obtained from our studies with

Table II. Assignment of Protonated ^{13}C Signals (ppm) of $d(ATGGGTACCCAT)_2$ Duplex without and with Zn^{2+} [a]

	Zn^{2+}/duplex		
carbons	0[d]	1	8
A_1C8	142.4	142.3	142.5
A_7C8	141.2 (142.0)	141.2	141.7
$A_{11}C8$	141.7	141.7	142.0
A_1C2	154.5	154.5	154.5
A_7C2	154.8 (154.5)	154.5	154.7
$A_{11}C2$	155.0	155.0	154.7
G_3C8	138.1	138.6	139.6
G_4C8	137.1 (137.6)	138.1	139.6
G_5C8	136.9	137.0	137.3
T_2C6	138.7	138.9	139.0
T_6C6	138.0 (139.3)	138.3	138.5
$T_{12}C6$	138.9	139.0	139.0
C_8C6	141.7	141.9	142.2
C_9C6	142.2 (142.6)	142.7	143.1
$C_{10}C6$	142.9	143.0	143.1
C_8C5	98.1	98.1	98.0
C_9C5	98.3 (98.8)	98.3	98.2
$C_{10}C5$	98.8	98.7	98.7
T_2Cm[c]	14.0	13.9	14.2
T_6Cm	14.3 (14.8)	14.1	14.1
$T_{12}Cm$	14.2	14.2	14.3
A_1C1'	87.8	87.8	88.0
A_7C1'	84.7 (85.5)	85.0	
$A_{11}C1'$	85.4	85.5	v
G_3C1'	84.2	*b*	e
G_4C1'	84.2 (84.3)	84.8	r
G_5C1'	85.0	85.7	y
C_8C1'	86.5	86.5	
C_9C1'	86.7 (86.8)	87.2	b
$C_{10}C1'$	86.2	86.6	r
T_2C1'	85.6	85.9	o
T_6C1'	85.3 (86.1)	85.6	a
$T_{12}C1'$	85.4	85.6	d
A_1C3'	79.3	79.3	
A_7C3'	79.0 (80.1)	79.0	
$A_{11}C3'$	78.8	79.0	
G_3C3'	78.8	78.6	
G_4C3'	78.7 (78.9)	78.6	
G_5C3'	77.3	78.0	
C_8C3'	76.3	76.5	
C_9C3'	76.8 (76.7)	76.7	
$C_{10}C3'$	77.0	76.8	
T_2C3'	78.0	77.7	
T_6C3'	78.5 (78.9)	77.6	v
$T_{12}C3'$	71.0	71.6	e
A_1C4'	89.6	89.7	r
A_7C4'	87.2 (88.1)	87.5	y
$A_{11}C4'$	86.3	86.5	
G_3C4'	87.2	87.4	b
G_4C4'	86.6 (86.3)	86.8	r
G_5C4'	86.8	87.2	o
C_8C4'	85.3	85.5	a
C_9C4'	85.6 (86.0)	85.9	d
$C_{10}C4'$	86.3	86.6	
T_2C4'	85.8	86.2	
T_6C4'	85.6 (86.2)	86.0	
$T_{12}C4'$	86.5	86.7	
$A_1C5',5''$	64.0	64.5	

[a] Experimental conditions: 99.96% D_2O, pH 6.00 (uncorrected in D_2O) and 12 °C. [b] Data could not be obtained, since the cross peaks disappear. [c] T methyl carbon. [d] Data in parentheses from ref 12.

previous assignments.[12] In these tables, average values are given for a particular type of carbon in the center of the duplex. Most of the assignments were quite consistent. As expected for some carbons on both end-nucleotides, a few ppm chemical shift difference from the average for carbons of the same type in interior nucleotides was found. For example, the A_1C1' signal is 2.7 ppm downfield (+) from other AC1′ signals. Likewise the following differences were observed: A_1C4', +2.5 ppm; A_1C5, +1.3 ppm; A_1C8, +0.9 ppm; $T_{12}C3'$, −7 ppm (upfield).

From a comparison of base carbon chemical shifts without Zn^{2+} and with Zn^{2+} from Tables II and III, the most significant shifts

Table III. Assignment of Nonprotonated ^{13}C Signals (ppm) of $d(ATGGGTACCCAT)_2$ Duplex without and with Zn^{2+} [a]

	Zn^{2+}/duplex			Zn^{2+}/duplex	
carbons	0[c]	4.5	carbons	0[c]	4.5
A_1C4	150.5	150.4	$C_{10}C4$	167.9	167.4
A_7C4	150.7 (151.2)	150.7	T_2C2	153.2	153.0
$A_{11}C4$	150.7	150.8	T_6C2	152.3 (153.7)	152.2
A_1C5	121.7	121.6	$T_{12}C2$	153.5	153.4
A_7C5	120.2 (120.9)	120.0	T_2C4	168.7	168.4
$A_{11}C5$	120.5	120.4	T_6C4	168.7 (168.8)	168.4
A_1C6	158.3	158.6	$T_{12}C4$	168.7	168.4
A_7C6	158.0 (158.3)	158.3	G_3C4	153.1	*b*
$A_{11}C6$	158.0	158.3	G_4C4	152.6 (153.4)	*b*
C_8C2	158.7	158.4	G_5C4	152.4	152.8
C_9C2	159.0 (159.0)	158.8	G_3C5	117.5	116.8
$C_{10}C2$	159.0	158.8	G_4C5	117.5 (117.5)	116.8
C_8C4	167.2	166.8	G_5C5	117.5	117.2
C_9C4	167.9 (168.1)	167.4			

[a] Experimental conditions: 99.96% D_2O, pH 6.00 (uncorrected in D_2O) and 12 °C. [b] Data could not be obtained, since the signals are too broad to see the coupling. [c] Data in parentheses from ref 12.

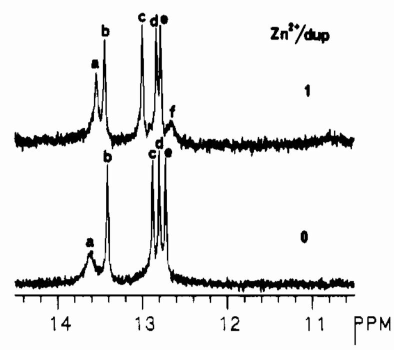

Figure 4. Imino proton NMR spectrum of $d(ATGGGTACCCAT)_2$ (30 mM in bases) at 23 °C, in H_2O (pH 6.0), without Zn^{2+} (bottom) and with 1 Zn^{2+}/duplex (top). The signals are labeled as follows: (a) T_2A_{11}; (b) T_6A_7; (c) G_4C_9; (d) G_3G_{10}; (e) G_5C_8; (f) A_1T_{12}.

are G_4C8 (2.5 ppm), G_3C8 (1.5 ppm), C_9C6 (0.7 ppm), G_3C5 (−0.7 ppm), and G_4C5 (−0.7 ppm). Of some interest, the T methyl ^{13}C shift pattern was altered by adding different amounts of Zn^{2+}. For instance, the order was from downfield to upfield T_6, T_{12}, T_2, T_{12}, T_6, T_2; and T_{12}, T_2, T_6 at $R_{Zn/duplex}$ = 0, 1, and 8, respectively, although the chemical shifts changed little.

Exchangeable Proton Signal Assignments and Temperature Dependence. Imino proton signals of the oligomer in 90% H_2O/10% D_2O were assigned by 1D NOE and thermal melting methods. Five peaks in the region of 10–15 ppm for the free self-complementary dodecamer (30 mM in bases) are visible in the 8 °C spectrum (not shown). The signal for the end base pair (A_1T_{12}) was not observed because of end fraying.

When the temperature was increased to 18 °C (Figure 4), the most downfield signal a shifted upfield. This signal, which shifted upfield further and disappeared as the temperature was increased to 30 °C, is assigned to the imino proton of T_2 in the penultimate base pair. The signal d at 12.83 ppm (at 18 °C) greatly lost its intensity by 40 °C and then essentially disappeared around 50 °C. This signal, which did not shift significantly with temperature, is assigned to the G_3 imino proton. The signal b at 13.44 ppm (at 18 °C) lost some intensity at about 40 °C. Above 55 °C the three remaining signals (b, c, and e) were broadened and disappeared simultaneously, suggesting that they were for central base pairs. On the basis of characteristic shifts, the upfield signals at 12.91 ppm (c) and 12.76 ppm (e) (at 18 °C) are assigned to G_4 and G_5, respectively, and the downfield signal (b) at 13.44 ppm (at 18 °C), to T_6. During the temperature increase to 55 °C, no signal was observed around 11–12 ppm, the region where hairpin imino signals are normally detected.[29]

(29) Hare, D. R.; Reid, B. R. *Biochemistry* **1986**, *25*, 5341.

1D NOE experiments confirmed the assignments. At 10 °C, when the signal assigned above to T_2A_{11} was irradiated, the signal assigned to the G_3C_{10} base pair gave an NOE effect, as did the signal assigned to $A_{12}H2$. When the imino signal of G_3C_{10} was irradiated, NOE's were observed for the imino signals of T_2A_{11} and the signal at 12.92 ppm, assigning it as G_4C_9. As expected, the G_3C_{10} and the G_5C_8 signals responded to G_4C_9 irradiation, the T_6A_7 and the G_4C_9 signals responded to G_5C_8 irradiation, and the A_7H2 and G_5C_8 imino signals responded to T_6A_7 irradiation.

In the presence of Zn^{2+} ($R_{Zn/duplex} = 1$; the oligomer concentration is 30 mM in bases), the shifts of the imino proton signals (assigned by NOE spectroscopy) were quite similar to those observed with no Zn^{2+} present. However, a broad and most upfield imino signal appeared at ~12.66 ppm at 18 °C (Figure 4); this sixth signal is assigned to the terminal base pair (A_1T_{12}). At 8 °C, this signal was underneath the three G imino proton signals. It shifted upfield when the temperature was increased and disappeared above 25 °C. On addition of Zn^{2+} at 18 °C, the imino signal of base pair G_4C_9 shifted from 12.91 to 13.00 ppm and that of G_5C_8 shifted from 12.76 to 12.78 ppm (Figure 4). The imino proton signal of T_2A_{11} became sharper and shifted upfield from 13.65 to 13.56 ppm on addition of 1 Zn^{2+}/duplex. When the temperature was increased, this signal shifted upfield further by ~0.2 ppm and disappeared above 30 °C. Simultaneously, the G_3C_{10} signal shifted upfield slightly and combined with the signal of G_5C_8. All signals broadened by 40 °C, especially for the T_6A_7 base pair, but the relative intensities of the signals remained essentially constant until 50 °C. Above 50 °C, the signals were broadened significantly and simultaneously. In comparison, the signal of G_3C_{10} had essentially disappeared for the no Zn^{2+} sample at 50 °C.

Temperature Dependence of the Nonexchangeable ^{1}H Signals. Variable-temperature studies of the oligomer were performed by monitoring the 1D NMR signals of the nonexchangeable protons, especially in the aromatic and T methyl proton regions, in D_2O.

When two conformational transitions accompany a temperature increase, the first transition is typically from duplex to hairpin, and the second, from hairpin to random coil.[30,31] In the absence of Zn^{2+}, the base proton signals of the oligomer gradually became complex as the temperature was increased (Figure 5a). Between 40 and 50 °C the number of signals appeared to have doubled and the intensities of the original signals to have decreased. We attribute these changes to a partial duplex-to-hairpin transition. From 50 to 60 °C, the signals remained broadened. However, above 65 °C, one set of sharp signals was apparent again. In the presence of 2.5 Zn^{2+}/duplex, only one set of signals was present from 22 to 75 °C. The signals became broad at ~55 °C but sharpened above 65 °C (Figure 5b).

The temperature dependences of the chemical shifts for selected base aromatic proton and the thymidine methyl resonances in the absence and presence of Zn^{2+} are shown in Figure 6–8. Although the assignments above 50 °C are difficult because of signal crossing and broadening, the Zn^{2+}-absent case was assigned by the EXSY experiment (see below) and the Zn^{2+}-present case was assigned by analogy.

The T_6H6 resonance in the absence of Zn^{2+} (Figure 6) exhibited an upfield shift with increasing temperature below the melting temperature. On the basis of previous studies,[32] this behavior suggests that a conformational transition in the middle of the strand precedes melting. However, in the presence of Zn^{2+}, this signal shifted upfield even more (Figure 8). The three CH6 resonances show a large downfield shift between 50 and 65 °C for the sample without Zn^{2+} (Figure 6) and between 55 and 70 °C for the sample with Zn^{2+} (Figure S2 (supplementary material)). Such C_6H6 downfield shifts are characteristic of the melting of a double-helical structure and have been observed in d-(CGCG),[33] d(CGCGCG),[33-35] and d(CGCGTTGTTCGCG).[32]

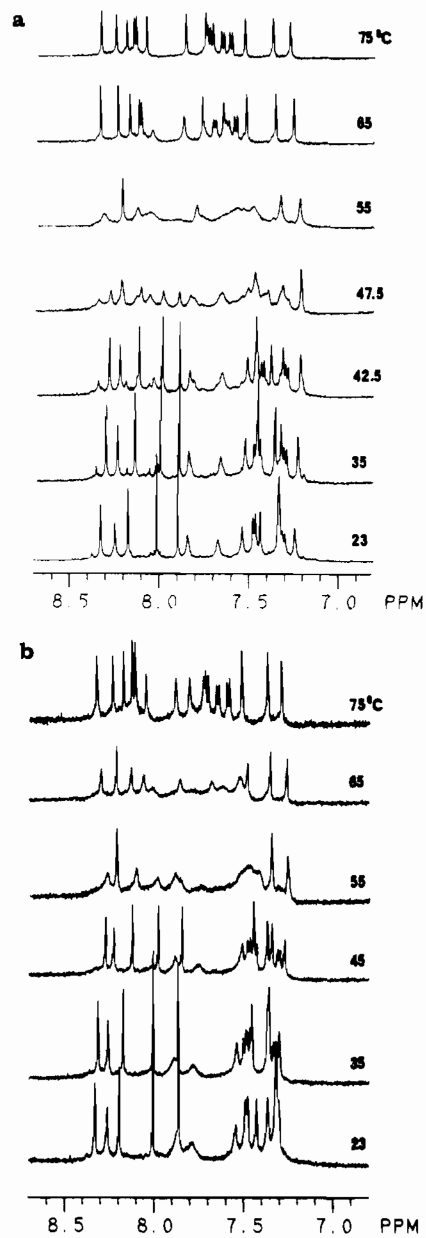

Figure 5. ^{1}H NMR spectra of $d(ATGGGTACCCAT)_2$ (30 mM in bases) in D_2O (pH 6.0, uncorrected) at different temperatures as indicated: (a) without Zn^{2+}; (b) with 1 Zn^{2+}/duplex.

For the three GH8 resonances, large downfield shifts occur for the no Zn^{2+} sample around 60 °C (Figure S3), but for the Zn^{2+} sample they occur above 70 °C (Figure S2). The chemical shift changes of the AH8 signals were quite similar in both samples with and without Zn^{2+}. When the temperature was increased, the AH8 signals shifted upfield by 0.03–0.1 ppm and then shifted downfield by about the same amount (Figures 6 and 8). For both samples, the inflection points were at ~50 °C for all of the AH8 signals and the final chemical shifts at 75–80 °C were similar to the room-temperature values.

In the TCH_3 spectral region in the absence of Zn^{2+}, weak signals from the hairpin form are observed at room temperature (Figure 7). These hairpin signals are shifted downfield with respect to the corresponding duplex signals. The signals from the duplex form shifted downfield with increasing temperature for both end

(30) Wemmer, D. E.; Chou, S. H.; Hare, D. R.; Reid, B. R. *Nucleic Acids Res.* **1985**, *13*, 3755.
(31) Roy, S.; Weinstein, S.; Borah, B.; Nickol, J.; Appella, E.; Sussman, J. L.; Miller, M.; Shindo, H.; Cohen, J. S. *Biochemistry* **1986**, *25*, 7417.
(32) Williamson, J. R.; Boxer, S. G. *Biochemistry* **1989**, *28*, 2819.
(33) Cheng, D. M.; Kan, L.; Frechet, D.; Ts'o, P. O. P.; Uesugi, S.; Shida, T.; Ikehara, M. *Biopolymers* **1984**, *23*, 775.
(34) Uesugi, S.; Shida, T.; Ikehara, M. *Chem. Pharm. Bull.* **1981**, *29*, 3573.
(35) Frechet, D.; Cheng, D. M.; Kan, L.; Ts'o, P. O. P. *Biochemistry* **1983**, *22*, 5194.

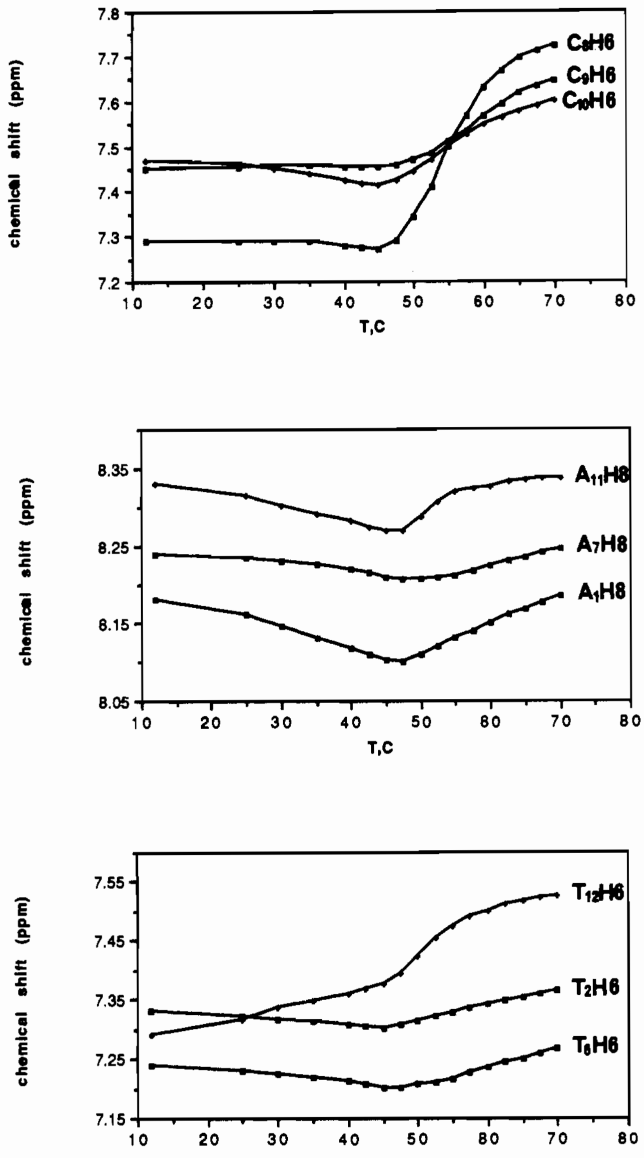

Figure 6. Chemical shift dependence on temperature of selected base protons of d(ATGGGTACCCAT)$_2$ (30 mM in bases in D_2O, pH 6.0, uncorrected) as indicated.

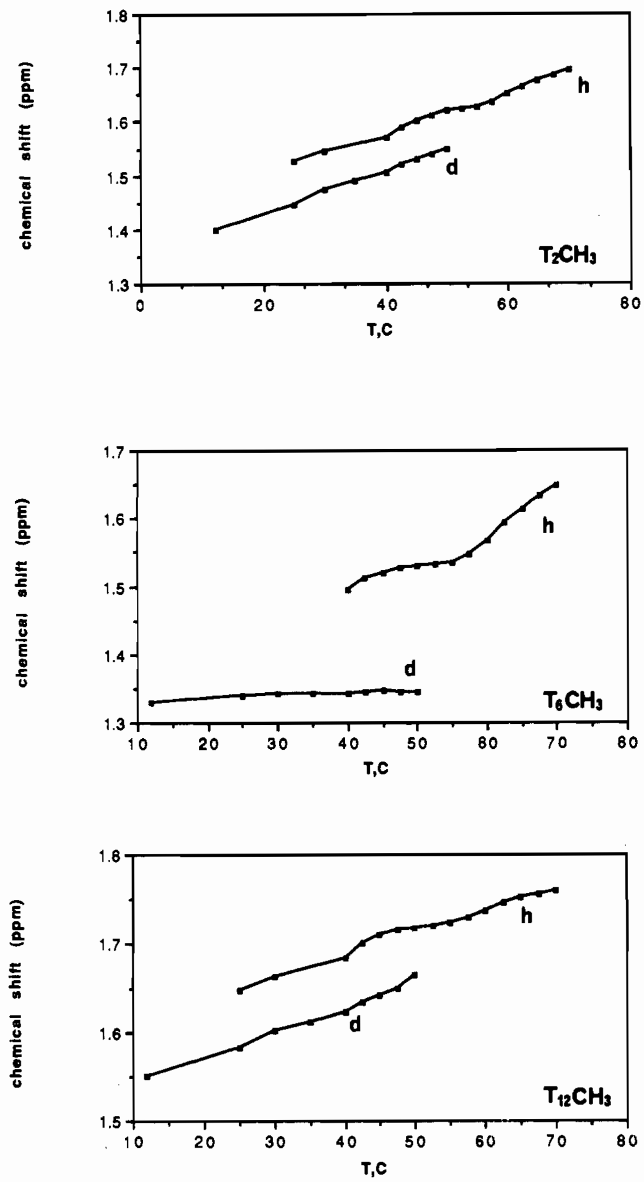

Figure 7. Chemical shift dependence on temperature of methyl protons of d(ATGGGTACCCAT)$_2$ (30 mM in bases in D_2O, pH 6.0, uncorrected) as indicated.

TCH_3 (T_2 and T_{12}). However, no shift for the T_6CH_3 signal was found up to ~50 °C. Above 50 °C the signals of the duplex and the hairpin forms merged. At this juncture, the shifts of the merged signals correlated with the hairpin form. With further increase in temperature, the signals shifted downfield further. The resulting biphasic curves suggest a transition from hairpin to coil forms in this second phase. This pattern is most obvious for T_6CH_3. In the presence of Zn^{2+}, most interestingly, the T_6CH_3 signal did not shift below 58 °C (Figure 8). Above 58 °C, a large downfield shift was observed to ~75 °C. No hairpin signals were observed at any temperature.

Hairpin Signal Identification. As we noted, in the absence of Zn^{2+} two forms were present, particularly in the temperature range 40–45 °C. An EXSY spectrum was obtained, therefore, at 42.5 °C in order to identify the signals of the hairpin form by chemical exchange with the duplex form (Figure 9). By this method, many of the signals of the hairpin were assigned (Table IV). The most significant differences in the chemical shifts between duplex and hairpin forms were found for the CH6 and CH5 signals. In contrast to other duplex and hairpin signals, which were similar, these were shifted from 0.2 to 0.7 ppm. Another large difference between the two forms was found for the A_7H2 signal, with the signal of the hairpin shifted downfield by 0.61 ppm relative to the duplex signal. These hairpin signal assignments were very useful for assigning the signals of the coil form at high temperature.

Zn^+-Induced Hairpin to Duplex Transition. At low concentrations of the oligomer, for example 4 mM in bases, the imino proton spectrum at 20 °C (Figure 10) was quite different from that at high concentration (30 mM; see Figure 4). At low concentration, two downfield signals, 13.02 and 12.77 ppm, as well as one broad upfield signal at 10.83 ppm, are observed. The downfield signals are very likely from G imino protons in GC base pairs. The shift of the upfield signal is consistent with the imino proton of an unpaired thymidine in a loop region of a hairpin structure.[29] There are also two very small signals near 13.5 ppm and another two at ~12.9 ppm.

When 1 Zn^{2+}/duplex was added to the solution, the upfield signal became broader and smaller, the two downfield signals diminished, and at least five signals emerged in the downfield region. Two of these signals are probably due to an increase in size of the original two signals present at ~12.9 ppm before the addition of Zn^{2+}. Further downfield, two new overlapping peaks emerged at ~13.5 ppm (Figure 10). These overlapping signals appear to arise from the merging and increase in size of the two small signals originally at ~13.5 ppm. Obviously, the spectrum must be that for two forms, which are almost certainly a hairpin and a duplex. When more Zn^{2+} was added (2 Zn^{2+}/duplex in

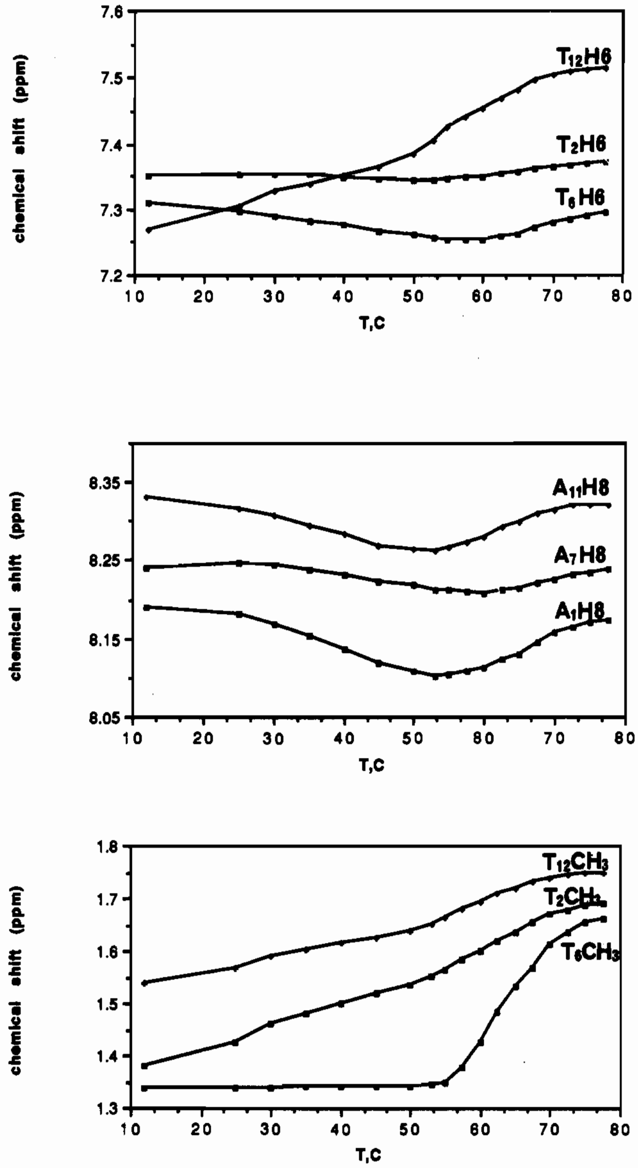

Figure 8. Chemical shift dependence on temperature of selected base and methyl protons of d(ATGGGTACCCAT)$_2$ (30 mM in bases in D_2O, pH 6.0, uncorrected) as indicated at 2.5 Zn^{2+}/duplex.

Table IV. ^1H Chemical Shifts (ppm) of d(ATGGGTACCCAT)$_2$ in Its Duplex, Hairpin, and Coil Forms[a]

protons	duplex[b]	hairpin[c]	coil[d]
A_1H8	8.11	8.12	8.19
A_7H8	8.21	8.18	8.25
$A_{11}H8$	8.27	8.33	8.33
A_1H2	7.97	8.02	8.08
A_7H2	7.45	8.06	8.14
$A_{11}H2$	7.88	8.03	8.15
G_3H8	7.82	7.80	7.86
G_4H8	7.65	7.66	7.75
G_5H8	7.50	7.53	7.71
T_2H6	7.30	7.32	7.37
T_6H6	7.22	7.21	7.28
$T_{12}H6$	7.37	7.45	7.53
C_8H6	7.27	7.67	7.61
C_9H6	7.46	7.64	7.65
$C_{10}H6$	7.42	7.53	7.73
C_8H5	5.25	5.95	6.00
C_9H5	5.46	5.90	5.98
$C_{10}H5$	5.62	5.84	5.86
T_2CH_3	1.45	1.52	1.70
T_6CH_3	1.35	1.44	1.66
$T_{12}CH_3$	1.59	1.66	1.76

[a] Experimental conditions: 99.96% D_2O, pH 6.00 (uncorrected in D_2O), temperature as noted. [b] At 12 °C. [c] At 42.5 °C. [d] At 75 °C.

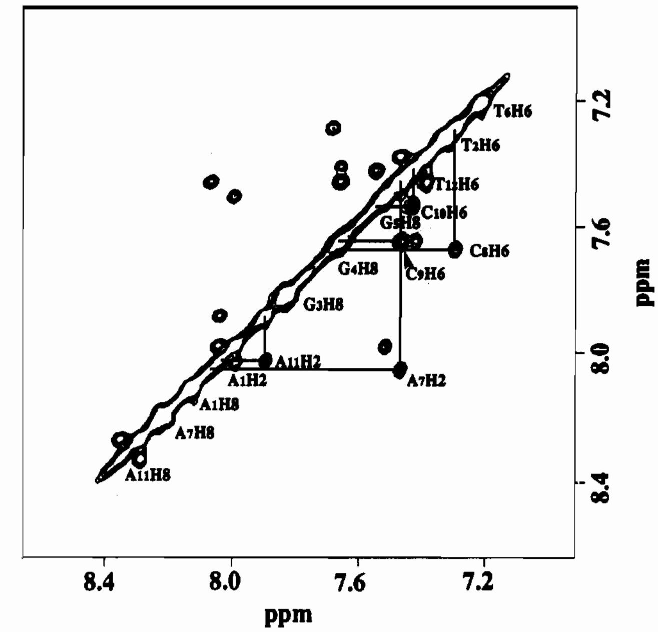

Figure 9. Expanded EXSY spectrum of the aromatic proton region of d(ATGGGTACCCAT)$_2$ (40 mM in bases in D_2O, pH 6, uncorrected) at 42.5 °C. The chemical exchange cross peaks between the duplex and hairpin forms are labeled and linked by solid lines, if they are far from the diagonal. NOE cross peaks are not labeled.

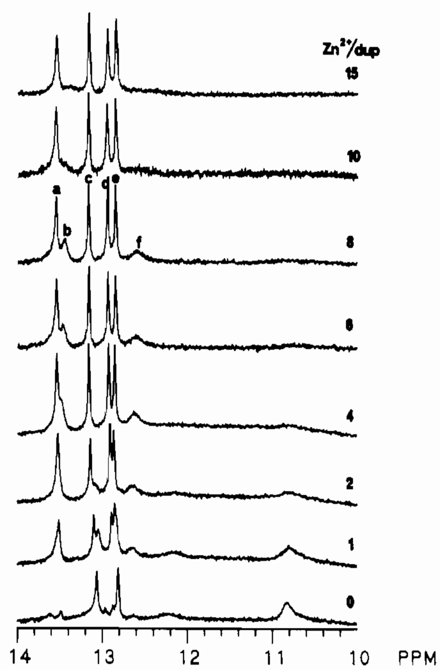

Figure 10. Imino proton NMR spectra of d(ATGGGTACCCAT)$_2$ (4 mM in bases) at 20 °C in H_2O (pH 6.0) at the indicated ratios of Zn^{2+} to duplex. The signals are labeled as follows: (a) T_6A_7; (b) T_2A_{11}; (c) G_4C_9; (d) G_3C_{10}; (e) G_5C_8; (f) A_1T_{12}.

total), the upfield signal was almost gone and the one set of signals that dominated was similar to that in the spectrum of the oligomer at high concentration. With further addition of Zn^{2+} at 20 °C, the upfield signal disappeared completely. At this stage, only duplex complexed with Zn^{2+} remained.

The spectral dependence on further addition of Zn^{2+} is interesting: One of the overlapping signals at 13.5, ppm shifted slightly, if at all, and remained sharp. We assign it to T_2A_{11} on the basis of this behavior as well as temperature studies discussed below. A signal at 12.60 ppm appeared (assigned to A_1T_{12}). When the Zn^{2+} titration at 20 °C reached 10 Zn^{2+}/duplex, the signals at 13.45 (T_2A_{11}) and 12.60 (A_1T_{12}) ppm became broad again and the sharp peak at 12.92 ppm, which we assign to the G_3C_{10} imino

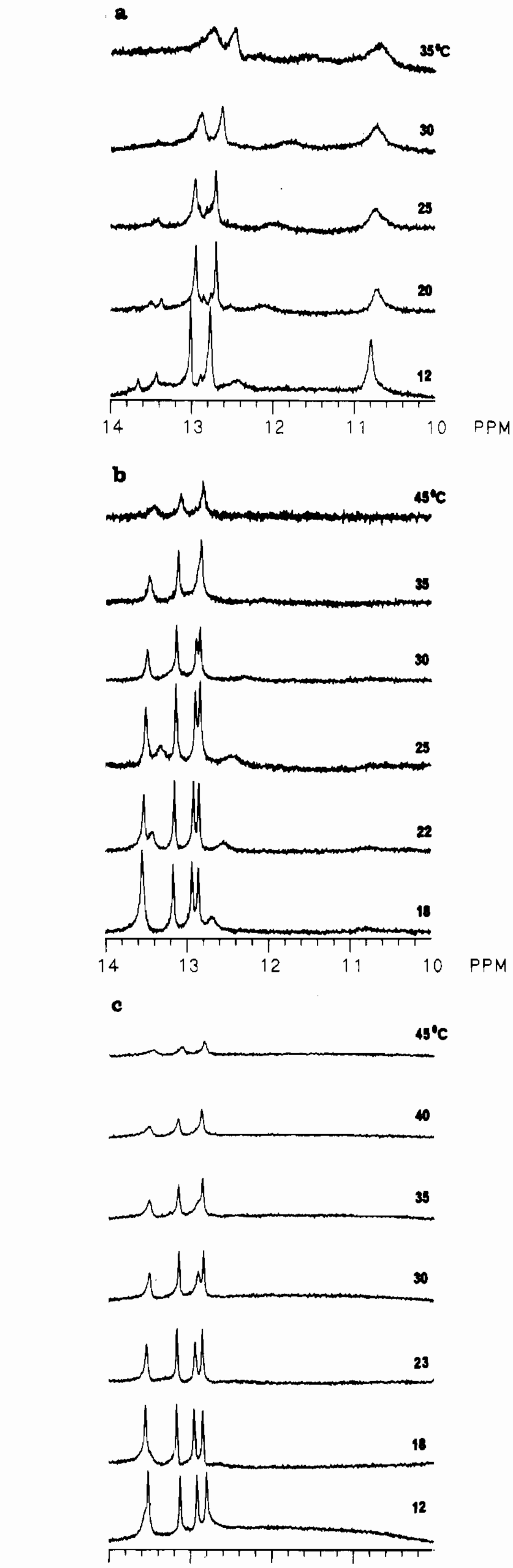

Figure 11. Imino proton NMR spectra of d(ATGGGTACCCAT)$_2$ (4 mM in bases) in H_2O (pH 6.0) at the temperatures indicated: (a) without Zn^{2+}; (b) with 4 Zn^{2+}/duplex; (c) with 10 Zn^{2+}/duplex.

proton, broadened slightly. An increase to 25 Zn^{2+}/duplex produced no further spectral change (Figure 10).

Temperature-dependence studies were performed at 0, 4, and 10 Zn^{2+}/duplex titration stages. For the sample without Zn^{2+} (Figure 11a), the upfield signal from the loop region became even broader above 20 °C, and the downfield sharp signals from the GC base pairs become broad above 25 °C. All peaks became very broad and were barely detectable over the noise above 45 °C. For the 4 Zn^{2+}/duplex sample (Figure 11b), presumably the most stable duplex form, the A_1T_{12} and T_2A_{11} base pair signals shifted upfield, indicating end fraying, with increase in temperature; these signals disappeared at ~30 °C. The T_6A_7 and G_3C_{10} signals became broad at 30 °C. Above 45 °C, the signals of all remaining base pairs were broadened. For the 10 Zn^{2+}/duplex sample (Figure 11c), the A_1T_{12} and T_2A_{11} base pairs had melted by 18 °C. The T_6A_7 and G_3C_{10} signals started to become broad even at 23 °C. Above 45 °C, the signals were extensively broadened.

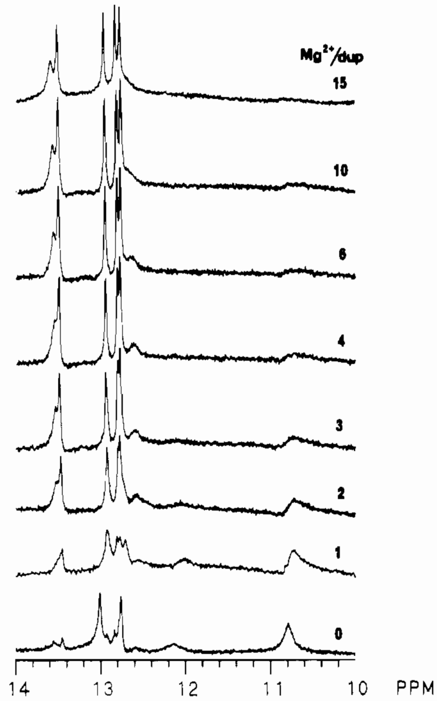

Figure 12. Imino proton NMR spectra of d(ATGGGTACCCAT)$_2$ (4 mM in bases) at 23 °C in H_2O (pH 6.0) at the indicated ratios of Mg^{2+} to duplex.

An analogous experiment was conducted on a similar 4 mM solution with Mg^{2+} at 23 °C. The upfield imino signal of T_6 in the loop broadened, but the extent of broadening was less than in the Zn^{2+} titration; the signal does not essentially disappear until addition of 4 Mg^{2+}/duplex (Figure 12). On the basis of the disappearance of the hairpin signals and the formation of signals characteristic of the duplex form, Zn^{2+} appears qualitatively to be twice as effective as Mg^{2+} in stabilizing the duplex form. One notable difference in the imino region is a less pronounced downfield shift of the G_4 imino signal on duplex formation. The shift value of 13.0 ppm can be compared to a value of 12.9 ppm for the duplex in a concentrated solution and to 13.2 ppm for the Zn^{2+} titration of the dilute sample. Another major difference is that the imino signal of the penultimate base pair, T_2A_{11}, did not broaden and shift upfield as in the Zn^{2+} case; instead, the signal shifted slightly downfield, remaining broad up to 15 Mg^{2+}/duplex. Finally, the broad signal for the terminal base pair moved downfield and beneath the G_3 and G_5 signals up to this ratio of added Mg^{2+}.

The temperature dependence of the imino proton spectrum of the Mg^{2+} $R = 10$ sample was indicative of melting from the ends followed by disruption at the center of the duplex. The spectral changes (not shown) were qualitatively similar to the $R = 10$ Zn^{2+} experiment except that, in the Mg^{2+} case, the melting temperature was about 10 °C higher.

^{31}P NMR Spectroscopy. The ^{31}P NMR spectrum of the oligomer consists of five sharp peaks and several overlapping signals between −3.94 and −4.50 ppm at 25 °C. The addition of Zn^{2+} ($R_{Zn/duplex} = 1$–8) made the resonances slightly broader and shifted signals upfield by ca. 0.05–0.15 ppm (at $R = 8$, signals were between −4.03 and −4.63 ppm). No new peak was observed.

When the temperature of the $R = 0$ sample was increased, the signals were broadened with loss of resolution; for example, at 42.5 °C the signals were between −3.96 and −4.43 ppm. However, at 67.5 °C almost all signals were overlapped between −3.87 and −4.15 ppm. In the presence of Zn^{2+}, $R = 2.5$, the temperature influence was similar to that noted with $R = 0$ except that the degree of the signal overlap was even greater than that without Zn^{2+} (figures not shown). A more dilute sample, 4 mM in base, gave two large signals at −4.1 and −4.4 in the normal range and a small upfield signal at ca. −4.9 ppm.

Discussion

The insight we have gained from our NMR studies will be discussed first with regard to the nature of the premelt species, then to the hairpin-to-duplex equilibrium, and finally to the melting process.

One of the clearest results from the ^1H NMR study is that, even at relatively low ratios, Zn^{2+} binds to N7 of G. There are essentially no significant shifts of the AH8 signals. Furthermore, the G_5H8 signal is not affected by Zn^{2+} addition. The major shifts are at G_4H8 and G_3H8. The ^{13}C NMR data strongly support this conclusion. There are no appreciable shifts of the G_5 or any A ^{13}C signals, and the shift pattern of the G_3 and G_4 signals is that expected on the basis of studies of monomers.[11] This result indicates that there is a significant selectivity in the binding of a simple metal ion to DNA bases. Pullman and Pullman have shown that a run of three adjacent G's has the most attractive molecular electrostatic potential (MEP) of all possible three-base sequences of DNA.[17] If the Zn^{2+} is a simple reporter of electrostatic attraction, this result suggests that the central G is the most electronegative of the three bases, followed by the 5′G and finally the 3′G. Indeed, the order of MEP is G*G*G > T*G*G > G*G*T,[17,18] in agreement with our findings.

It has been suggested that two adjacent G's could form either a metal sandwich complex[36] or a GN7–M–GN7[37] cross-linked species. These types of adducts could explain the shifts of the H8 signals of both G_3 and G_4. However, since the lone pair on N7 lies in the plane of the base, a good binding interaction requires that the plane of the bases form an acute dihedral angle. Such acute angles are found in crystal structures of many bis nucleotide and nucleoside complexes[37,38] and even in limited X-ray structural reports of metal-bound oligonucleotides.[39] This type of structure is quite disruptive of DNA conformation. We found no appreciable changes in relative NOE cross-peak intensities on addition of Zn^{2+}. Thus, a N7–Zn–N7 chelate structure or the chemically unreasonable GMG sandwich structure is not observed by ^1H NMR studies of nonexchangeable proton signals.

Further evidence that such cross-linked or sandwich structures are unlikely comes from our studies of the exchangeable imino proton signals. The shifts of these signals are quite sensitive to H-bonding interactions, and the widths are sensitive to exchange, as found, for example, by Reedijk in an N7–Pt–N7 cross-linked adduct.[40] In our study, there are no appreciable changes in shifts or line widths of the G imino signals at low R values, where the ^{13}C shifts are large. Thus, a disrupted conformation is unlikely.

A characteristic feature of N7–M–N7 cross-linked species is a more open C5′O-P–OC3′ bond angle to accommodate the strain. We and others have shown that N7–Pt–N7 cross-linked adducts induced significant downfield shifts of the signal of the phosphate group between the two G's.[41] No such shift was observed, thus providing further evidence against a cross-link. We predict that a sandwich structure would also open this C5′O–P–OC3′ angle and should lead to an appreciable downfield shift of the ^{31}P NMR signal. Although such a sandwich complex has not been observed to verify this prediction, intercalators such as metalloporphyrins induce large downfield shifts.[9] Our ^{31}P NMR results are not consistent with the sandwich or cross-linked species.

A sandwich-type species would have a different electronic perturbation on the base than an N7-bound species. Thus, the ^{13}C NMR chemical shift change pattern characteristic of an N7-bound electrophile is unlikely to occur for a sandwich complex. Furthermore, the strain induced in either the sandwich or cross-linked structure would alter the conformation of one or both of the G_3 or G_4 sugar moieties. For example, the 5′ sugar in Pt(II)–GpG cross-linked species has an N conformation, which would lead to readily detected ^{13}C shifts.[13] No significant changes in shifts were observed for the sugar ^{13}C signals, suggesting no appreciable change in sugar conformation. Therefore, the ^{13}C spectral results also are inconsistent with either a cross-linked or sandwich species.

Another type of adduct that has been proposed includes N7/PO_4 chelation.[15] The sterically most feasible such chelate would be formed by interaction of the metal with the 5′-phosphate of the nucleotide. Such a chelate cannot form unless the sugar pucker is in the N conformation.[42] We have shown that the ^{13}C NMR signals of the deoxyribose shift considerably for an S-to-N conformational change.[43] An approximately 8 ppm upfield shift is expected for C3′.[13] We found no appreciable C3′ shifts of the G residues and conclude that a chelate is unlikely.

There is also no indication from ^{31}P NMR shifts of strong interaction with the phosphate groups. At present, the extent of shift induced by a directly coordinated Zn^{2+} cannot be predicted. Relatively large downfield shifts of ~10 ppm of ^{31}P NMR signals have been found for N7/αPO_4 chelates with 5′-nucleoside monophosphates, but phosphodiesters did not form such chelates.[42] On the basis of this evidence, formation of a chelate complex appears very unlikely.

The ^{13}C signals of C8 and C5 of the G_3 and G_4 bases are shifted in the downfield and upfield directions, respectively, characteristic of N7 binding.[11] Such large shifts are unlikely to be due to outer-sphere interactions and are comparable to shifts we have observed when Pt(II) (a stronger electrophile than Zn^{2+}) is bound to N7 of cross-linked bases.[43] As Zn^{2+} concentration was increased, signals of both G_3 and G_4 continued to shift to about the same relative extent, considering the precision of the measurements. Thus, we believe that, at either of the two equivalent GGG regions of a duplex, the Zn^{2+} is binding either at G_3N7 or at G_4N7 but not at both sites. Models also suggest that two adjacent N7-bound Zn^{2+} species are not possible.

The relatively minor effects of high levels of Zn^{2+} on the imino signals argues against any significant transfer of the GN1 proton to CN3 in the complementary base. Stronger evidence that this proton transfer is not occurring can be found in the ^{13}C NMR data. Protonation of N3 of cytidine characteristically leads to large upfield shifts of C4 and C2 (6–8 ppm), moderate downfield shifts of C6, and small shifts of C5 and C1′.[11] For C_9 and C_{10}, C2 shifts upfield by 0.2 ppm and C4 by 0.5 ppm, while C5 shifts upfield by 0.1 ppm and C6 and C1′ shift downfield by an average of ~0.5 ppm. This shift pattern, when compared to that for cytidine, is consistent with a somewhat stronger protonation of

(36) Richard H.; Schreiber, J. P.; Daune, M. *Biopolymers* **1973**, *12*, 1.
(37) Miller, S. K.; VanDerveer, D. G.; Marzilli, L. G. *J. Am. Chem. Soc.* **1985**, *107*, 1048.
(38) Lippert, B. *Prog. Inorg. Chem.* **1989**, *37*, 1. Chiang, C. C.; Sorrell, T.; Kistenmacher, T. J.; Marzilli, L. G. *J. Am. Chem. Soc.* **1978**, *100*, 5102. Poojary, M. D.; Monohar, H. *J. Chem. Soc., Chem. Commun.* **1982**, 533. Goodgame, D. M. L.; Jeeves, I.; Reynolds, C. D.; Skapski, A. C. *Nucl. Acids Res.* **1975**, *2*, 1375.
(39) Admiraal, G.; van der Veer, J.; de Graaff, R. A.; den Hartog, J. H. J.; Reedijk, J. *J. Am. Chem. Soc.* **1987**, *109*, 592. Sherman, S. E.; Gibson, D.; Wang, A. H.-J.; Lippard, S. J. *J. Am. Chem. Soc.* **1988**, *110*, 7368.
(40) den Hartog, J. H. J.; Altona, C.; van Boom, J. H.; van der Marel, G. A.; Haasnoot, C. A. G.; Reedijk, J. *J. Am. Chem. Soc.* **1984**, *106*, 1528.
(41) Caradonna, J. P.; Lippard, S. J. *Inorg. Chem.* **1988**, *27*, 1454 and references cited therein. Kline, T. P.; Marzilli, L. G.; Live, D.; Zon, G. *J. Am. Chem. Soc.* **1989**, *111*, 7057 and references cited therein. Fouts, C. S.; Marzilli, L. G.; Byrd, R. A.; Summers, M. F.; Zon, G.; Shinozuka, K. *Inorg. Chem.* **1988**, *27*, 366. den Hartog, J. H. J.; Altona, C.; van Boom J. H.; van der Marel, G. A.; Haasnoot, C. A. G.; Reedijk, J. *J. Biomol. Struct. Dyn.* **1985**, *2*, 1137.
(42) Reily, M. D.; Marzilli, L. G. *J. Am. Chem. Soc.* **1986**, *108*, 8299. Reily, M. D.; Hambley, T. W.; Marzilli, L. G. *J. Am. Chem. Soc.* **1988**, *110*, 2999. Alessio, E.; Xu, Y.; Cauci, S.; Mestroni, G.; Quadrifoglio, F.; Viglino, P.; Marzilli, L. G. *J. Am. Chem. Soc.* **1989**, *111*, 7068.
(43) Mukundan, S.; Xu, Y.; Zon, G.; Marzilli, L. G. To be published.

N3, but any definitive conclusion must await further study. The only G signal that shifts substantially on deprotonation is C2,[11] which can not be observed by our methods. However, clearly there is not substantial proton transfer to N3.

In addition to the spectral features discussed above, there are shifts, mostly minor, suggestive of small conformational changes on addition of Zn^{2+}. The largest change is for G_3H1'. These changes could be due to local effects produced by Zn^{2+} binding to G_3 or G_4. The relatively few changes in the NOE cross-peak intensities on addition of Zn^{2+} are also consistent with negligible "global" conformational changes.

Small NOE changes involving AH2 could be due to sliding in of propellar-twisted base pairs.[44] The decrease in these NOE cross peaks for the end A residues on addition of Zn^{2+} suggests a more normal B-form structure. However, the A_7H_2 to C_8H1'NOE cross peak increases slightly.

In the absence of Zn^{2+} and, especially, at $\sim$40 °C, there is a second form that we believe is the hairpin species, since it is favored by lowering the concentration. To further explore this species, we are currently studying a similar sequence but with a mismatch, which will favor the hairpin form. Preliminary reults confirm that the minor species we observe here is a hairpin. Furthermore, UV melting studies and electrophoresis studies support the formation of a hairpin. An imino signal is readily observed at $\sim$11 ppm, consistent with the presence of T in a hairpin loop. This hairpin is unusual in that the 3'- and 5'-ends are AT rich. The propensity to form a hairpin may be related to the presence of the three adjacent G residues. It has been shown that the sequence 5'-PyTTPu-3' leads to a two base pair loop with PyPu base pairing, but the sequence 5'-PuTTPy-3' gives a four base pair loop.[45] As predicted by these studies, our evidence is most consistent with a four base pair loop. However, we have an A in the loop that destabilizes two base pair loops.[45]

At relatively low ratios of Zn^{2+}/strand, the hairpin form is converted to the duplex form, as evidenced by the loss of the imino signal at 11 ppm and the emergence of imino signals characteristic of the duplex form dominant at higher concentrations. Ongoing UV studies suggest that Zn^{2+} also kinetically promotes formation of the duplex form. At higher concentrations and higher temperatures, some of the nonexchangeable proton signals of the hairpin form can be detected. An EXSY spectrum allowed us to assign many of the base signals using the duplex assignments (Table IV). Some of the largest downfield shifts accompanying the duplex-to-hairpin transition involved A_7H2, C_8H6, C_8H5, and C_9H5; smaller shifts were observed for $C_{10}H5$, C_9H6, and $C_{10}H6$. These downfield shifts suggest the greatest difference between the stem region and the duplex involves the 3'-end of the oligonucleotide. This pattern is found for clearly established duplex-to-hairpin transitions; for $d(C_1G_2C_3G_4T_5A_6T_7A_8C_9G_{10}C_{11}G_{12})$, the A_6H2 and A_8H2 signals shift by $\sim$0.75 ppm and C_9H5 by $\sim$0.3 ppm, with lesser shifts of C_9H6.[30] Shifts for other signals were smaller.

The lack of downfield shifts for T_6 suggests that this base is still stacked with G_5. Consistent with this view, on conversion of the hairpin form to the coil form, the G_5H8 signal undergoes a larger downfield shift on formation of the coil form than the other two G H8 signals. Also, the T_6CH_3 signal undergoes a large downfield shift when the hairpin is converted to the coil form (Table IV). Stacking of loop bases on the 5'-side to the stem base is a characteristic feature of hairpins.[32]

In the presence of Zn^{2+}, however, no evidence was found for the hairpin form in the more concentrated sample. The change in chemical shift with temperature, in this case, suggests that Zn^{2+} at low ratios stabilizes the duplex. This finding is in keeping with the suggestion that one of the roles of Zn^{2+} in facilitating the renaturation of DNA melted in the presence of Zn^{2+} is the prevention of the formation of structures such as hairpins.[16]

Characteristically, metal ions such as Zn^{2+} lower T_m for DNA at high ratios of added metal ion.[1,2,14] The 12-mer we have studied is probably too short to provide insight into this phenomenon. On the basis of the exchangeable proton signals, at low levels of Zn^{2+} the AT ends are stabilized to exchange but as the Zn^{2+} ratio was increased, the AT ends became destabilized with end fraying evidenced by upfield shifts of the A_1T_{12} and T_2A_{11} imino signals. The shifts of the imino signals of the central base pairs were not greatly affected by these high levels of Zn^{2+}. However, the line widths of the imino signals of these base pairs were affected, particularly G_3C_{10} and T_6A_7. The former base pair is toward the end, and the broadening of its signal before the G_4C_9 and G_5C_8 signals might be expected. However, clearly the central AT base pair is destabilized. Such central base pair destabilization was observed when the duplex (at 4 mM) was melted in the presence of Mg^{2+}. In the Mg^{2+} experiment, a $T_m \sim 10$ °C higher than in the Zn^{2+} experiment was found. We believe that the lower T_m's at high metal ratios are probably best explained by Zn^{2+} stabilizing the coil form by binding to sites exposed by base unpairing. The Mg^{2+} cation appears to stabilize the AT ends of the duplex to a greater extent than the Zn^{2+} cation. However, our results presented here and kinetic studies (unpublished) demonstrate that Zn^{2+} is more effective than Mg^{2+} in converting the hairpin form to the duplex form. We do not understand the reasons for these differences.

The similar T_m values of DNA, regardless of GC content, at high R for Cu^{2+} and the similarity of these T_m values to that of poly[(dAdT)]$_2$ led to the suggestion that only the AT regions were responsible for the melting of DNAs; i.e., the Cu^{2+} had melted out the GC regions.[46] However, the temperature dependence of the imino proton spectrum (Figure 11c) demonstrates that the GC regions are stabilized with respect to the AT regions at high levels of Zn^{2+}. Although a longer oligonucleotide must be studied to reach a definite conclusion about preferential AT base pair melting, it is clear, as we recently suggested,[16] that GC base pairs are not dissociated when Zn^{2+} binds. Base pair melting is favored by high Zn^{2+} for both AT and GC base pairs. The paramagnetic Cu^{2+} ion cannot be studied by the methods used here. However, the similar effects of Cu^{2+} and Zn^{2+} on DNA properties suggest strongly that Cu^{2+} also does not melt out GC base pairs.

In summary, our NMR studies demonstrate that it is feasible to obtain useful information about binding of labile metal ions to DNA using ^{13}C NMR spectroscopy of oligonucleotides. Our results provide strong evidence for GN7 coordination and for selective interaction to some G residues over others. No evidence of coordination to A residues was found. This sequence selectivity may reflect primarily electrostatic attraction, but more work is needed to understand it. At low ratios of Zn^{2+} to duplex, the binding of Zn^{2+} to N7 appears to stabilize the duplex form without significantly altering H-bonding interactions or promoting the transfer of the GN1 H to CN3. At the oligonucleotide level, there is no major global change in DNA conformation. No evidence was found for any significant change in sugar pucker, ruling out an N7,phosphate chelate. Although the ^{31}P NMR results do not rule out direct Zn^{2+}–phosphate interactions (only small shifts are found), they do rule out any large local conformational change such as would accompany the formation of N7–Zn–N7 cross-links. Of additional interest, Zn^{2+} seems to be particularly effective at stabilizing the duplex and coil forms at the expense of the hairpin form in the oligonucleotide studied here. The oligonucleotide studied here forms a hairpin to an appreciable extent only at low concentrations, where detailed NMR studies are not possible. General conclusions concerning Zn^{2+}–hairpin interactions must await studies with oligonucleotides having other sequences. Since Zn^{2+} is representative of the effects of divalent metal ions on DNA structure and stability, we believe that our studies have implications for metal ions other than Zn^{2+} and suggest that cross-linked or sandwich species are not formed by Cu^{2+} either.

Acknowledgment. We thank the National Institutes of Health

(44) Chou, S.-H.; Flynn, P.; Reid, B. *Biochemistry* **1989**, *28*, 2422.
(45) Blommers, M. J. J.; Walters, J. A. L. I.; Haasnoot, C. A. G.; Aelen, J. M. A.; van der Marel, G. A.; van Boom, J. H.; Hilbers, C. W. *Biochemistry* **1989**, *28*, 7491.
(46) Hiai, S. *J. Mol. Biol.* **1965**, *11*, 672.

for support through Grant GM 29222 to L.G.M. and Prof. David Live for helpful suggestions. We appreciate grants from the National Institutes of Health and the National Science Foundation toward the purchase of the NMR spectrometers.

Registry No. d(ATGGGTACCCAT), 130306-96-6; Zn, 7440-66-6; Mg, 7439-95-4.

Supplementary Material Available: Tables of complete assignments of ^1H NMR data (Tables SI–SIII) and figures of the HMQC experiment with 1 Zn^{2+}/duplex and of the chemical shift dependence on temperature of the signals of selected base protons (Figures S2 and S3) (6 pages). Ordering information is given on any current masthead page.

Contribution from the Department of Inorganic and Physical Chemistry, Indian Institute of Science, Bangalore 560 012, India

Octabromotetraphenylporphyrin and Its Metal Derivatives: Electronic Structure and Electrochemical Properties

P. Bhyrappa and V. Krishnan*,†

Received March 7, 1990

The free-base octabromotetraphenylporphyrin (H_2OBP) has been prepared by a novel bromination reaction of (*meso*-tetraphenylporphyrinato)copper(II). The metal [$V^{IV}O$, Co(II), Ni(II), Cu(II), Zn(II), Pd(II), Ag(II), Pt(II)] derivatives exhibit interesting electronic spectral features and electrochemical redox properties. The electron-withdrawing bromine substituents at the pyrrole carbons in H_2OBP and M(OBP) derivatives produce remarkable red shifts in the Soret (50 nm) and visible bands (100 nm) of the porphyrin. The low magnitude of protonation constants (pK_3 = 2.6 and pK_4 = 1.75) and the large red-shifted Soret and visible absorption bands make the octabromoporphyrin unique. The effect of electronegative bromine substituents at the peripheral positions of the porphyrin has been quantitatively analyzed by using the four-orbital approach of Gouterman. A comparison of MO parameters of MOBP derivatives with those of the meso-substituted tetraphenylporphyrin (M(TPP)) and unsubstituted porphine (M(P)) derivatives provides an explanation for the unusual spectral features. The configuration interaction matrix element of the M(OBP) derivatives is found to be the lowest among the known substituted porphyrins, indicating delocalization of ring charge caused by the increase in conjugation of p orbitals of the bromine onto the ring orbitals. The electron-transfer reactivities of the porphyrins have been dramatically altered by the peripheral bromine substituents, producing large anodic shifts in the ring and metal-centered redox potentials. The increase in anodic shift in the reduction potential of M(OBP)s relative to M(TPP)s is found to be large (550 mV) compared to the shift in the oxidation potential (300 mV). These shifts are interpreted in terms of the resonance and inductive interactions of the bromine substituents.

Introduction

In recent years there has been an increasing interest in the study of high-valent perhalogenated metalloporphyrins for catalytic epoxidation and hydroxylation reactions of organic substrates. The high-valent metalloporphyrin derivatives in the presence of oxygen donors such as PhIO, H_2O_2, NaOCl, $KHSO_5$, or RCOOOH function as efficient catalysts in the epoxidation of organic substrates.[1] The effectivenes of these catalysts has been traced to the stereochemical features of the porphyrins and their stability toward oxidative degradation in the presence of strong oxygen donors. It has been shown that the substitution of electron-withdrawing groups (cyano or bromo) at the pyrrole positions causes an anodic shift in the ring oxidation and reduction potentials of the porphyrins.[2] The interesting catalytic properties of the halogenated porphyrins offer a scope to study the electronic structure and other features of the metal derivatives of these porphyrins.

The halogen-substituted porphyrins so far reported fall into two classes—halogens appended either at the pyrrole positions[3] or at the *meso*-aryl groups[4] of the porphyrins. The porphyrin that has the halogen substitution both at the pyrrole and *meso*-aryl groups is a tetrakis(2,6-dichlorophenyl)octabromohemin derivative.[5] The latter compound has been found to be an efficient catalyst in the epoxidation reactions of olefins. Here, we report a novel method of synthesis of 2,3,7,8,12,13,17,18-octabromo-5,10,15,20-tetraphenyl-21,23(*H*)-porphyrin (H_2OBP) (Figure 1) through the bromination reaction of (5,10,15,20-tetraphenylporphyrinato)copper(II) (Cu(TPP)) and its subsequent demetalation by treatment with acid. The electronic spectral and magnetic resonance features of the various $V^{IV}O$, Co(II), Ni(II), Cu(II), Pd(II), Pt(II), Zn(II), and Ag(II) derivatives of H_2OBP have provided important structural information on these porphyrins. The electrochemical redox behavior of the free-base H_2OBP and its metal derivatives exhibits several interesting features. The present study illustrates the influence of peripheral bromine substituents on the electronic structure and electrochemical properties of the octabromoporphyrin derivatives.

Experimental Section

Materials. 5,10,15,20-Tetraphenylporphyrin (H_2TPP) was prepared according to the method of Rothemund et al.[6] and purified according to the procedure of Barnett et al.[7] Copper tetraphenylporphyrin (Cu(TPP)) was synthesized and purified by using reported procedure.[8] All solvents employed in the present study are of spectral grade and were distilled before use. Liquid bromine procured from Ranbaxy and basic alumina obtained from Acmes were used as received. The metal salts used in the preparation of octabromoporphyrin derivatives are given below. Copper(II) acetate monohydrate, zinc(II) acetate dihydrate, cobalt(II) acetate tetrahydrate, nickel(II) acetate tetrahydrate, and silver(I) acetate were procured from BDH and used without further purification. Palladium(II) chloride obtained from Ranbaxy was used as received. Dichloro(cyclooctadiene)platinum(II)[9] and bis(2,4-pentanedionato)oxovanadium(IV)[10] were prepared according to the reported procedures.

Synthesis of 2,3,7,8,12,13,17,18-Octabromo-5,10,15,20-tetraphenylporphyrin (H_2OBP). This was obtained by the bromination reaction of

† Associated with the Jawaharlal Nehru Centre for Advanced Scientific Research, Indian Institute of Science Campus, Bangalore, India.

(1) Renoud, J. P.; Battioni, P.; Bartoli, J. F.; Mansuy, D. *J. Chem. Soc., Chem. Commun.* **1985**, 888. Bruice, T. C.; Ostovic, D. *J. Am. Chem. Soc.* **1988**, *110*, 6906. Meunier, B. *Bull. Soc. Chim. Fr.* **1983**, 4578.
(2) Giradeau, A.; Callot, H. J.; Gross, M. *Inorg. Chem.* **1979**, *18*, 201. Giradeau, A.; Callot, H. J.; Jordan, J.; Ezhar, I.; Gross, M. *J. Am. Chem. Soc.* **1979**, *101*, 3857. Giradeau, A.; Ezhar, I.; Gross, M.; Callot, H. J.; Jordan, J. *Bioelec. Bioenerg.* **1976**, *3*, 519. Giraudeau, A.; Lovati, A.; Callot, H. J.; Gross, M. *Inorg. Chem.* **1979**, *20*, 769.
(3) Callot, H. J. *Bull. Soc. Chim. Fr.* **1974**, *8*, 1492. Callot, H. J. *Tetrahedron Lett.* **1973**, 1487.
(4) Traylor, P. S.; Dolphin, D.; Traylor, T. G. *J. Chem. Soc., Chem. Commun.* **1984**, 279.
(5) Traylor, T. G.; Tsuchiya, S. *Inorg. Chem.* **1987**, *26*, 1338.
(6) Rothemund, P.; Menotti, A. R. *J. Am. Chem. Soc.* **1948**, *70*, 1808.
(7) Barnett, G. H.; Hudson, M. F.; Smith, K. M. *Tetrahedron Lett.* **1973**, *30*, 2887.
(8) Dorough, G. D.; Miller, J. R.; Huennekens, F. M. *J. Am. Chem. Soc.* **1951**, *73*, 4315.
(9) Drew, D.; Doyle, J. R. In *Inorganic Synthesis*; Cotton, F. A., Ed.; Wiley: New York, 1972; Vol. XIII, p 48.
(10) Rowe, R. A.; Jones, M. M. In *Inorganic Synthesis*; Cotton, F. A., Ed.; Wiley: New York, 1957; Vol. V, p 114.

0020-1669/91/1330-0239$02.50/0 © 1991 American Chemical Society